

Thermal Modeling Of Industrial Environments Using Transient 0D And 1D Models.

Jordi VERA^{1,2*}, Octavi PAVON², Assensi OLIVA^{1,2}, Deniz KIZILDAG¹, Oriol SANMARTÍ¹, Domingo ALCALÁ³,

¹ Heat and Mass Transfer Technological Center (CTTC), Universitat Politècnica de Catalunya –
BarcelonaTech (UPC),
Terrassa (Barcelona), Spain
E-mail: cttc@cttc.upc.edu

² Termo Fluids S.L.,
Sabadell (Barcelona), Spain
E-mail: jordiv@termofluids.com

³ COCEDA, S.L. ,
El Prat de Llobregat (Barcelona), Spain
E-mail:

* Corresponding Author (jordi.vera.fernandez@upc.edu)

ABSTRACT

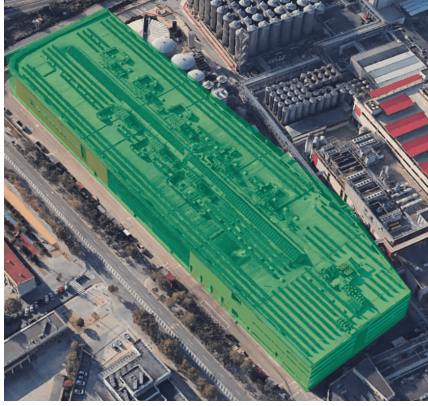
This work presents a fast and simplified numerical model designed to simulate the temporal evolution of temperature and humidity within industrial and residential buildings. A case study of an industrial plant in Spain is examined to understand its thermal dynamics and enhance staff comfort, particularly during high summer temperatures. The model integrates historical data of external temperature and solar radiation as boundary conditions to capture external influences on the plant's temperature. With transient box models, the simulation can predict temperature and humidity variations within the plant, considering factors such as wall composition, orientation, and solar radiation impact. The model also accounts for the ventilation system and internal heat generation from machinery, providing a comprehensive representation of thermal interactions within the industrial environment. Calibration of the model against experimental data demonstrates its accuracy in predicting temperature profiles within the plant. Detailed insights into wall temperature distributions, heat balances, and overall building heat contributions are obtained, offering valuable information for optimizing building comfort and energy efficiency.

1. INTRODUCTION

This work presents a fast and simplified model designed to simulate the temporal evolution of temperature and humidity within buildings of industrial and residential applications. A particular case is studied considering the beer manufacturing industrial plant of COCEDA, S.L. in Spain (Figure 1).

Understanding thermal dynamics in industrial facilities is crucial for maintaining staff comfort and operational efficiency. Many industrial plants face significant challenges in managing internal temperatures, especially during the summer months when external temperatures and solar radiation can cause substantial heat buildup. Despite the existing studies on thermal management in industrial settings, there is still a need for comprehensive models that integrate external and internal factors to predict temperature and humidity variations accurately. This study aims to fill this gap by developing a detailed and practical simulation model for thermal dynamics in an industrial plant. In addition, the results are compared to existing experimental data that validate the accuracy of the model.

The simulation employs transient box models to solve the heat equation, offering a practical approach to predicting temperature and humidity variations within the industrial setting. A 1D transient equation is used to address the complexities of different walls and layers of materials, considering factors such as orientation and solar radiation impact. Additionally, the model accounts for the inclusion of glass surfaces (Figure 1b), that have a great impact in the studied plant.



(a) Aerial view of the plant



(b) Glass Facade

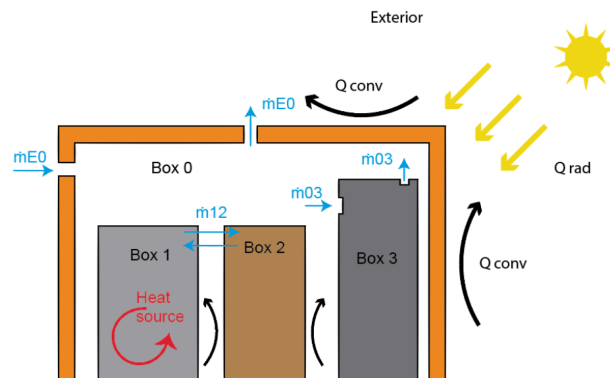
Figure 1: COCEDA, S.L. beer manufacturing plant

The ventilation system is a critical aspect of the simulation, modeled with a similar control methodology as the overall plant. The plant does not have air conditioning and uses a free cooling approach for the summer. Furthermore, the model includes the internal dynamics of the industrial plant, incorporating the heat and humidity generation from internal machines, and the thermal inertia of possible internal elements. In summary, this work provides a valuable contribution by offering a fast and simplified simulation model that captures the temporal evolution of temperature and humidity in an industrial plant. The inclusion of external conditions, detailed treatment of walls and windows, modeling of the ventilation system, and consideration of internal machine dynamics collectively contribute to a more accurate representation of the complex thermal interactions within the industrial environment.

2. NUMERICAL MODEL

2.1 Box model

The numerical model consists on a given number of boxes to describe the different regions on the plant. A schematic of this methodology is shown in Figure 2.

**Figure 2:** Box model

Each box is modelled using a 0D transient equation.

$$\rho c_p \frac{dT_i}{dt} V = \sum \dot{m}_{ij} c_p (T_j - T_i) + \sum_{\text{wall}} \dot{Q}_{\text{conv } ij} + \dot{Q}_{\text{source}, i} + \dot{Q}_{\text{ext}, i} \quad (1)$$

The interaction between a box i and a box j can be with a mass transfer \dot{m}_{ij} , or a convection heat transfer $\dot{Q}_{\text{conv } ij}$. Each box can have a source term $\dot{Q}_{\text{source}, i}$ that models the working machines, heating elements, people, etc. The boxes that

are in contact with the exterior have an additional term $\dot{Q}_{\text{ext}, i}$ to account for the heat transfer through the wall. Each box can be bounded by several exterior walls. Each wall can have a different material composition, thickness, solar absorptivity, thermal emissivity and orientation in reference to the sun.

Given that each box can have a given number K walls, the total heat contribution will be the summation of each wall.

$$\dot{Q}_{\text{ext}, i} = \sum_{k=1}^{K \text{ walls}} \dot{q}_{\text{ext}, ik} \cdot S_k \quad (2)$$

The term $\dot{q}_{\text{ext}, ik}$ corresponds to the contribution of each wall and is more detailed in 2.2. The term S_k is the wall surface.

2.2 External wall model

Special focus is given to the exterior wall heat balance. The model of walls is shown in Figure 3

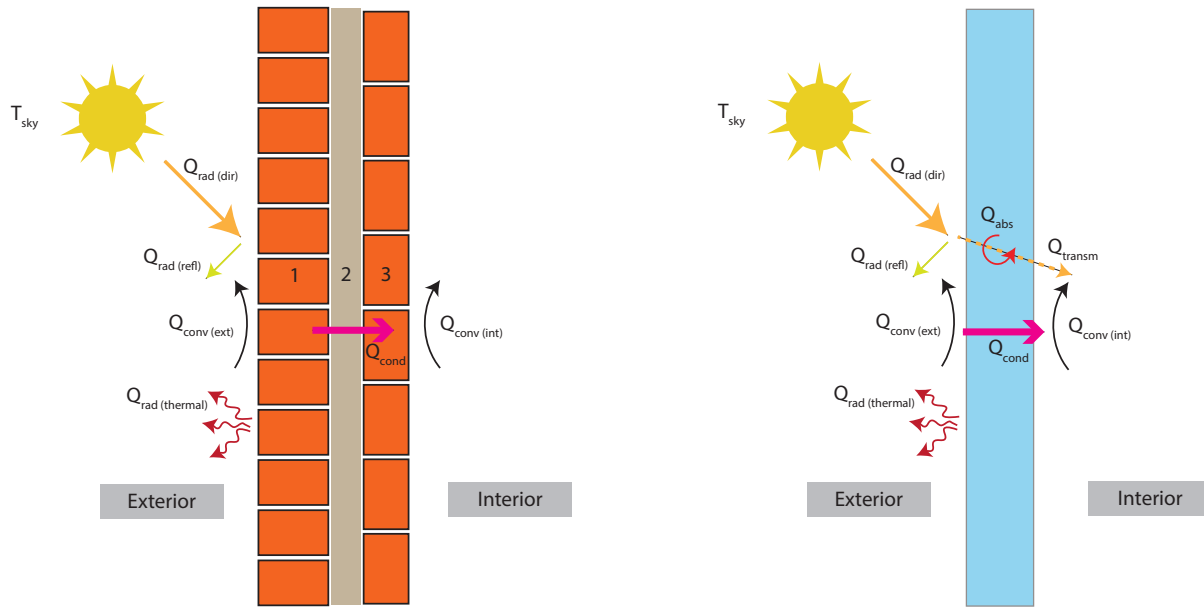


Figure 3: Heat balance at the wall. Left : opaque multi-layer wall, Right : Transparent wall

First the **Opaque multi-layer wall** case is considered. The exterior wall receive incident solar radiation that depends on the hour of the day, time of the year, wall orientation, and weather. Part of this solar radiation is reflected and part is absorbed depending on the surface reflectivity \mathcal{R} . This exterior wall also has a thermal radiation heat transfer that depends on the sky temperature of the surroundings, and the thermal emissivity of the surface. Finally the wall has a convection heat transfer to the exterior.

$$\dot{q}_{\text{ext}} = \alpha_{\text{ext}}(T_{\text{ext}} - T_{\text{wall,ext}}) + \sigma\varepsilon(T_{\text{sky}}^4 - T_{\text{wall,ext}}) + (1 - \mathcal{R}) \cdot \dot{q}_{\text{rad}} \quad (3)$$

The heat from the exterior is transferred via conduction over the wall to the interior, where it heats the air of the room via convection, as shown in equation (4).

$$\dot{q}_{\text{ext}} \rightarrow \rho c_p \frac{\partial T}{\partial t} = \lambda \frac{\partial^2 T}{\partial x^2} + \dot{q}_v \rightarrow \dot{q}_{\text{int}} = \alpha_{\text{int}}(T_{\text{wall,int}} - T_{\text{box}}) \quad (4)$$

This \dot{q}_{int} is the final contribution of the exterior and wall to the box. For each box i and wall k , this term will be $\dot{q}_{\text{ext}, ik}$ of equation (2).

The convection coefficients are calculated using empirical correlations. For free convection:

$$\text{Nu} = C(\text{Gr} \cdot \text{Pr})^m \quad \text{Gr} = \frac{g\beta(T_w - T_\infty)x^3}{\nu^2} \quad (5)$$

The parameters C and M depend on the geometry and flow regime. Table 1 summarizes the constant values for the different geometries and fluid regime of the studied box geometry.

Table 1: Correlation constant values

Geometry	$\text{Gr} \cdot \text{Pr}$	C	m
Vertical planes	$10^4 - 10^9$	0.59	$\frac{1}{4}$
	$10^9 - 10^{13}$	0.10	$\frac{1}{3}$
Upper surface of heated plates	$2 \cdot 10^4 - 8 \cdot 10^6$	0.15	$\frac{1}{3}$
	$8 \cdot 10^6 - 10^{11}$	0.15	$\frac{1}{3}$
Lower surface of heated plates	$10^5 - 10^{11}$	0.27	$\frac{1}{4}$

For isothermal turbulent vertical planes (the facades), the expressions from (Bayley, 1955) or (Warner & Arpaci, 1968) are used. For isothermal horizontal surfaces (the roof) correlations from (Fujii & Imura, 1972) (Lloyd & Moran, 1974) are used. A more extended table for different geometries can be found in (Holman, 2010).

The conduction equation of the solid wall is spatially discretized (Figure 4) using N nodes.

$$\rho c_p \frac{\partial T}{\partial t} = \lambda \frac{\partial^2 T}{\partial x^2} + \dot{q}_v \quad \rightarrow \quad \rho c_p \frac{\partial T}{\partial t} = \lambda_w \frac{T_{i-1} - T_i}{\Delta x^2} + \lambda_e \frac{T_{i+1} - T_i}{\Delta x^2} + \dot{q}_v \quad (6)$$

The thermal conductivity is calculated for each wall using the harmonic mean

$$\lambda_w = \frac{2}{\frac{1}{\lambda_{i-1}} + \frac{1}{\lambda_i}} \quad \lambda_e = \frac{2}{\frac{1}{\lambda_{i+1}} + \frac{1}{\lambda_i}} \quad (7)$$

The transient term is discretized using a backward Euler implicit method.

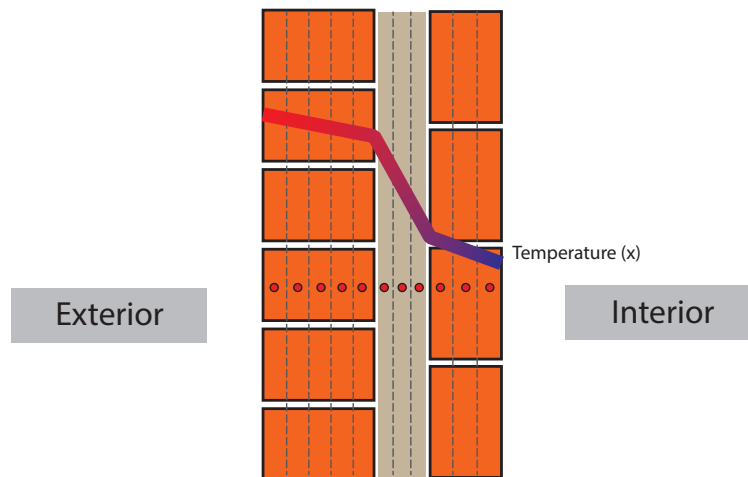


Figure 4: One dimensional wall discretization

The modelling of the **transparent wall** in the proposed model is very similar to the multi-layer opaque wall, but a main difference is considered. The incident solar radiation balance at the surface has an additional transmissivity term

\mathcal{T} . So now the wall absorptivity is not $\mathcal{A} = 1 - \mathcal{R}$ but:

$$\mathcal{A} = 1 - (\mathcal{R} + \mathcal{T}) \quad (8)$$

The absorbed solar heat is uniformly distributed as an internal wall source term instead of being applied at the surface. The transmitted solar heat is directly applied to the box source term.

2.3 Thermal inertia of the internal elements

The thermal inertia of the internal elements play a key role in the transient behaviour of the temperature profile. The characterization of the internal thermal inertia requires an accurate level of detail and information of all the internal elements and process. Although this detailed characterization is ideal regarding the accuracy, it requires a quantity of information that might be time consuming to gather.

In the studied case, some simplifications that reduce the required information, maintaining an acceptable level of accuracy and model simplicity are preferred. An assumption is made where the temperature of all the elements of a box (air and internal elements) is considered at equilibrium. This assumption is valid as long as the temperature changes over time (order of hours) are much slower than the heat transfer between internal elements and the air. The transient term then can be converted to:

$$\rho c_p \frac{\partial T}{\partial t} \rightarrow ((\rho c_p)_{\text{air}} + \sum (\rho c_p)_{\text{other}}) \frac{\partial T}{\partial t} \quad (9)$$

The characterization of the term: $(\rho c_p)_{\text{other}}$ can be done at different levels of detail depending on the known information. For example if a process requires a high volume of water that is stored in the plant, this mass and thermal properties can be added. Or if the weight and material of a machine or internal structure is known, it could also be added.

In the studied case the parameter $(\rho c_p)_{\text{other}}$ is unknown. Its value is determined with the calibration of the experimental results. The specific heat is set to $c_p = 2000 \text{ J/(kg} \cdot \text{K)}$ as a mean of typical construction materials, metals, and water and the occupation of a typical industrial plant should be between $50 - 500 \text{ kg/m}^2$.

2.4 Humidity evaluation

The water content mixed with air within a box is defined as m_w [kg]. The ratio w of water to dry air m_{da} [kg] and the vapor volumetric concentration φ are:

$$w = \frac{m_w}{m_{\text{da}}} \quad \varphi = \frac{m_w}{\mathcal{V}} \quad (10)$$

where \mathcal{V} is the box volume in m^3 . The governing equation of the water content evolution a ventilated box i with mass exchange with up to N boxes is presented.

$$\frac{dm_{w,i}}{dt} = \mathcal{S}_{w,i} + \sum_{j=1}^N (\dot{m}_{ij} \cdot (w_j - w_i)) \quad (11)$$

Where \mathcal{S}_w in kg/s is a humidity source (e.g. machines, people) inside the box, \dot{m}_{ij} is the mass flow of dry air, w_i the water content (mass) of the studied box, and w_i the water content of the box with air mass exchange (that can include the exterior domain).

This equation is temporally discretized and solved similarly to the heat equation with a backward Euler implicit method.

With the temperature T_i and water content w_i , the relative humidity can easily be calculated. The saturation pressure of water can be calculated using the August equation:

$$p_{\text{sat}} [\text{Pa}] = 133.32 \cdot \exp \left(20.386 - \frac{5132}{T} \right) \quad T \text{ in Kelvins} \quad (12)$$

The partial pressure of the water vapor can be calculated as:

$$p [\text{Pa}] = 461.5 \cdot \frac{m_w [\text{kg}]}{\mathcal{V} [\text{m}^3]} \cdot T [\text{K}] \leq p_{\text{sat}} \quad (13)$$

Finally, the relative humidity is calculated as:

$$\%RH = 100 \cdot \frac{p}{p_{\text{sat}}} \quad (14)$$

The energy equation (1) is for dry air and is valid as long as there are no important water content variations between inlet-outlets and as long as the relative weight of the sources is small. If these variations are important, it is more convenient to use the specific enthalpy h (equation (15))

$$\rho \frac{dh_i}{dt} V = \sum \dot{m}_{ij} (h_j - h_i) + \sum_{\text{wall}} \dot{Q}_{\text{conv } ij} + \dot{Q}_{\text{source, i}} + \dot{Q}_{\text{ext, i}} \quad (15)$$

For moist air, the enthalpy is calculated as a function of the water ratio w and temperature T .

$$h[\text{J/kg air}] = 1005 \cdot T[\text{°C}] + w \cdot 1000 \cdot (1.88 \cdot T[\text{°C}] + 2501) \quad (16)$$

Then the temperature can be calculated back with the inverse expression.

3. INDUSTRIAL PLANT CHARACTERIZATION

3.1 Geometry and orientation

Figure 5 shows the dimensions of the plant, the orientation, type of materials, and considered division of boxes.

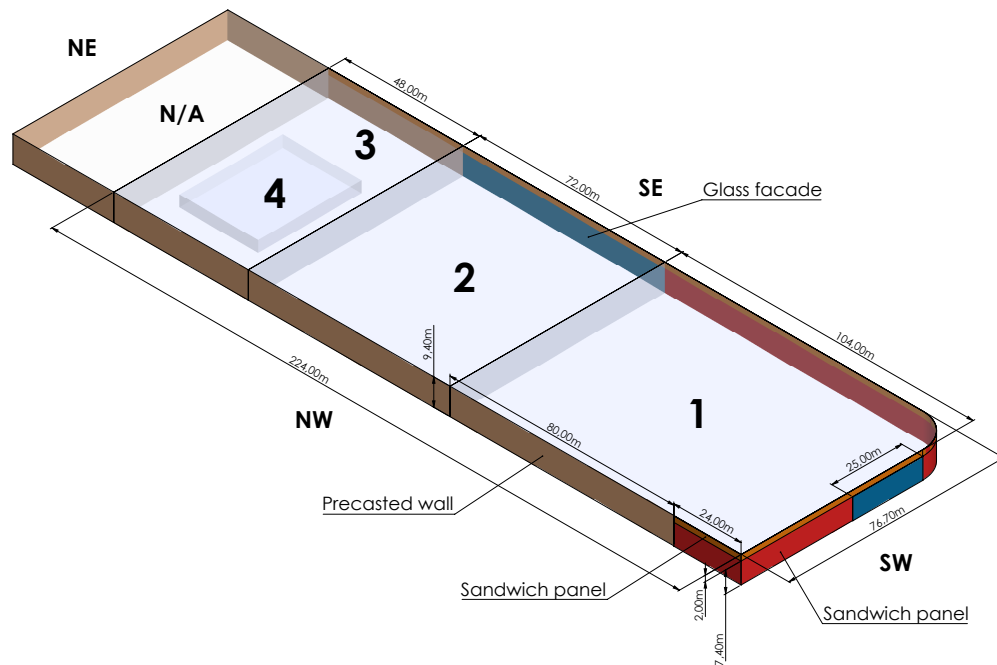


Figure 5: Facade characterization and dimensions

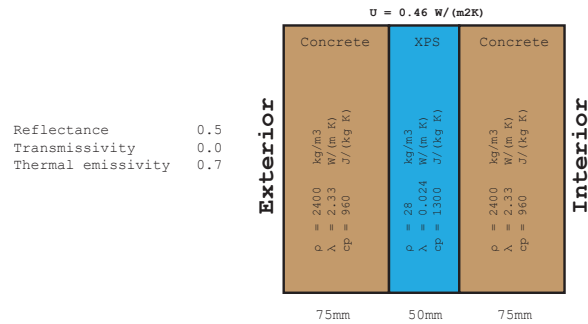
3.2 Ventilation control

The ventilation on summer is done using a free cooling approach. If the exterior temperature is lower than the interior one, the free cooling is activated. The maximum ventilation capacity of the plant is $483000 \text{ m}^3/\text{h}$. In the model, the working point will be set as 60% of this maximum ventilation capacity. Some sections of the plant (specially near the places with more human work activity) have additional local refrigeration units. The contribution of these units can be modelled with a negative source term on the heat equation of the corresponding box.

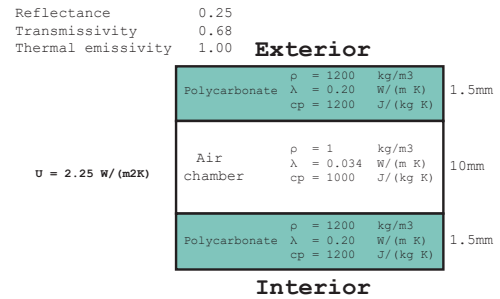
3.3 Material characteristics

Figure 6 presents the material characteristics considered for each boundary in both walls and roof.

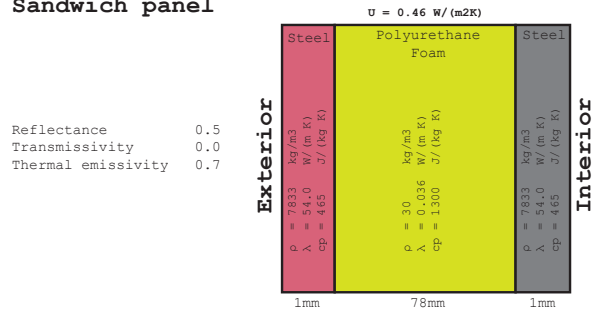
Precast concrete facade



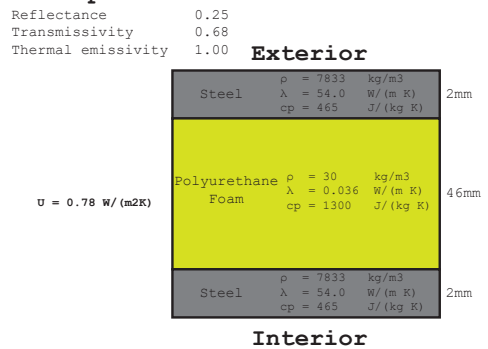
Rooflights



Sandwich panel



Roof sandwich panel



Glass facade

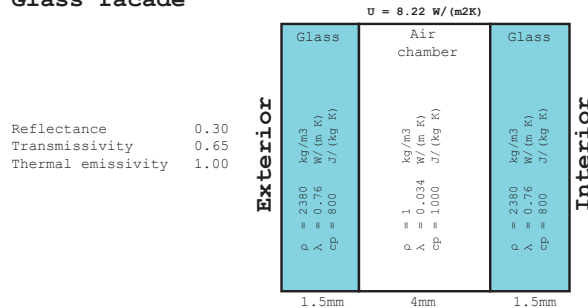


Figure 6: Material characteristics for the different boundary walls

3.4 External conditions

The model is input the following external conditions over time

- Incident solar radiation
- Exterior temperature
- Sky temperature

This external conditions can be either taken for a statistically typical year, to perform general studies of heat transfer, refrigeration needs, and overall performance. External conditions can also be from a given year in particular, this is specially useful for model calibration. In the calibration case, data from the year 2023 (meteo.cat, 2023)

4. MODEL CALIBRATION AND RESULTS

A set of experimental points were taken over the summer of 2023. The model is slightly calibrated with the thermal inertia term described on Section 2.3. Figure 7 shows the temperature of the box over two weeks. This box only had one experimental point of data. The model results are bounded within $\pm 2^\circ\text{C}$ of the experimental data.

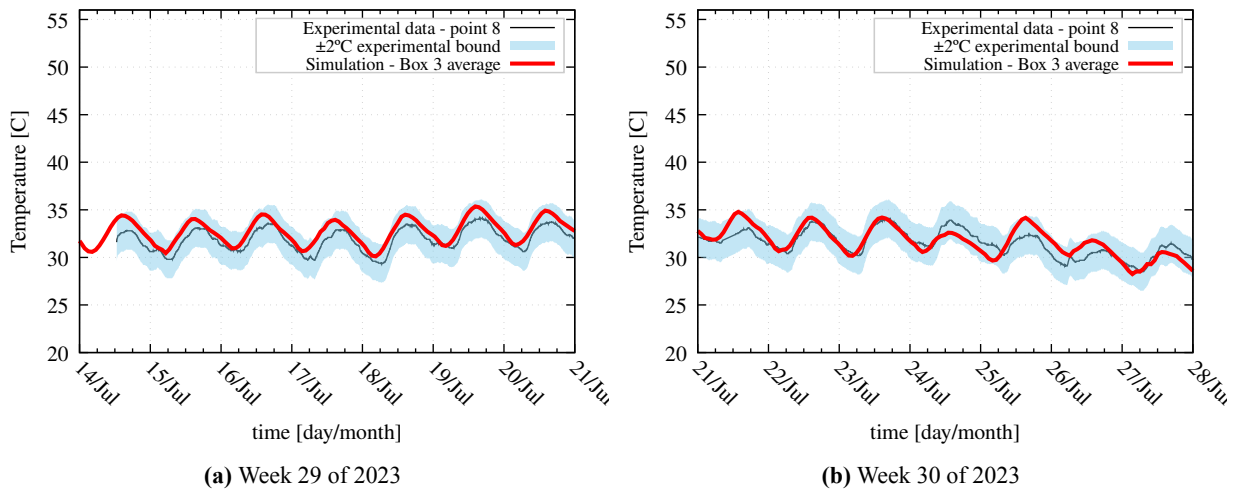


Figure 7: Temperature of box 1

Figure 8 shows the temperature evolution of box 2, compared to the three experimental points of that region. This box presents higher peaks of temperature because it is the one with the glass facade, having a high contribution of solar radiation. The model seems to correctly reproduce the behaviour and values of the peak temperature, with slight differences at the valleys, overestimating the temperature drop. Despite this small difference, the numerical model result is within the bounds defined with the minimum and maximum value of measured temperature.

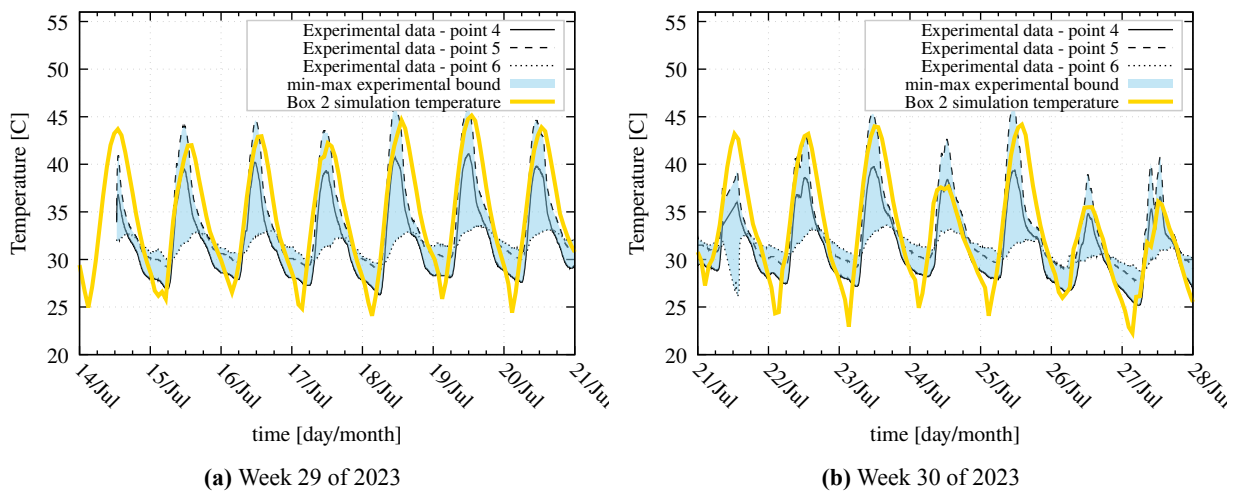


Figure 8: Temperature of box 2

Figure 9 shows the temperature evolution of box 3. This region has three experimental sensors. The results seem to be well bounded within the minimum and maximum experimental values.

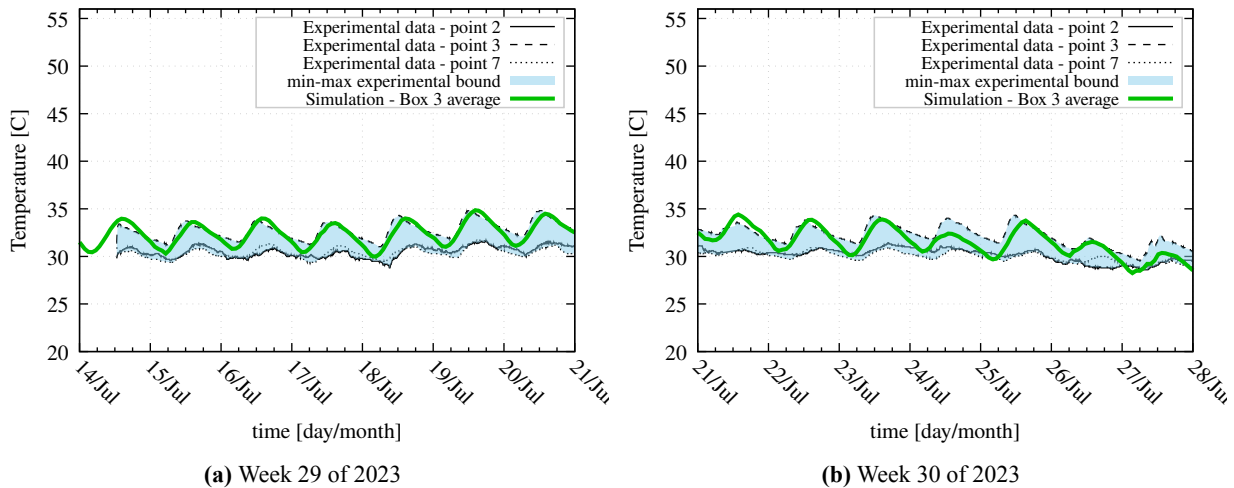


Figure 9: Temperature of box 3

The model can give a detailed insight of the thermal behaviour of the system. For example transient wall temperature distributions can be obtained. The temperature evolution over time for a NW oriented precast wall on a given day in July is shown in Figure 10.

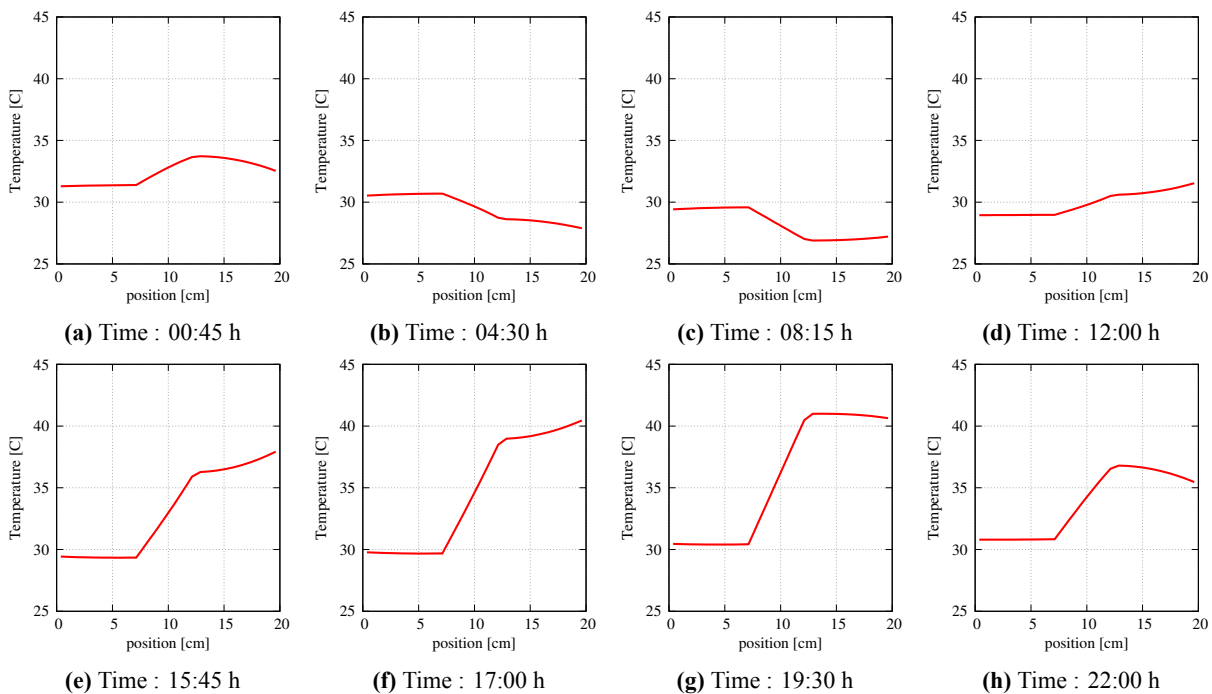
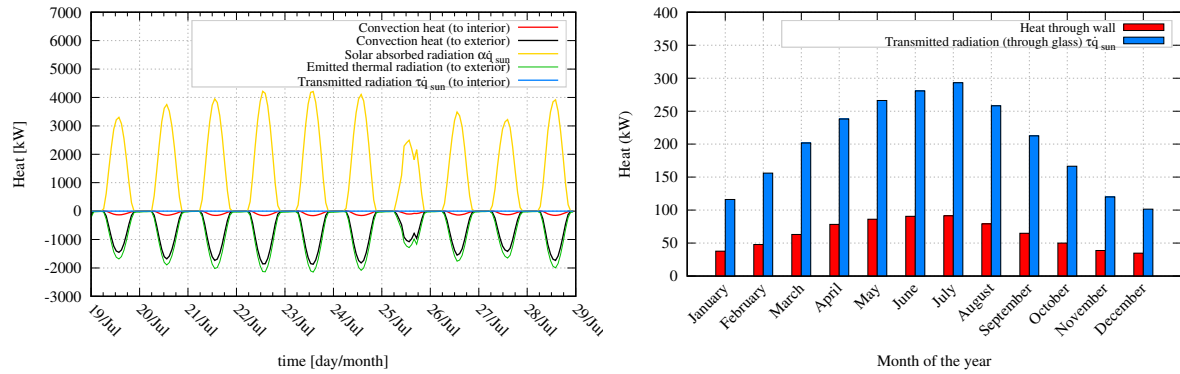


Figure 10: Temperature profile over time of a NW orientation, precast wall with XPS at the center. Internal face of the wall at $x = 0$ cm

The heat balance on a particular wall or surface (See Figure 3) can also be obtained. For example the roof sandwich panel heat balance is shown in Figure 11a. Overall heat balances of the building can also be studied. For example the contribution of the direct solar radiation transmitted through the glass surface, in comparison to the other heats, is shown in Figure 11b.



(a) Heat balance over time at the top roof for a typical day in July (b) Average heat received from the exterior through opaque and transparent walls for each month.

Figure 11: Heat balances over time

5. CONCLUSIONS

The 0D-1D transient coupled numerical model outlined in this paper offers a versatile tool for analyzing temperature dynamics in both industrial and residential settings. By incorporating environmental variables, internal heat sources, and ventilation systems, the model provides a comprehensive understanding of thermal behavior within buildings. Its robustness and computational efficiency make it a practical choice for engineers and researchers seeking to optimize building performance.

A practical example of the model is presented for the study of an industrial plant near Barcelona, Spain in a time frame of study over the 2023 summer. The numerical results were compared to the experimental data. This comparison showed that the temperature profiles (both values and transient variations) were properly reproduced, with some small differences that were within the expected uncertainty due to the simplifications of the model.

The transient temperature and heat value results provided by the model offer valuable insights into the thermal characteristics of building components, facilitating informed decision-making in design and operation. The simplicity of the model compared to other more complex approaches (like Computational Fluid Dynamics) makes it suitable for studying multiple cases with a low demand of computational power, allowing the user to perform parametric studies of different configurations. This information can lead to significant improvements in building comfort and energy efficiency, contributing to sustainable built environments.

REFERENCES

- Bayley, F. (1955). An analysis of turbulent free-convection heat-transfer. *Proceedings of the Institution of Mechanical Engineers*, 169(1), 361–370.
- Fujii, T., & Imura, H. (1972). Natural-convection heat transfer from a plate with arbitrary inclination. *International journal of heat and mass transfer*, 15(4), 755–767.
- Holman, J. P. (2010). *Heat transfer*. McGraw Hill Higher Education.
- Lloyd, J., & Moran, W. (1974). Natural convection adjacent to horizontal surface of various planforms. *Journal of Heat Transfer*, 96(4), 443–447.
- meteo.cat. (2023). *Servei meteorològic de catalunya, generalitat de catalunya*. <https://www.meteo.cat/>. (Accessed: 2024-04-04)
- Warner, C. Y., & Arpaci, V. S. (1968). An experimental investigation of turbulent natural convection in air at low pressure along a vertical heated flat plate. *International Journal of Heat and Mass Transfer*, 11(3), 397–406.